

Optical-mode-induced spin-lattice relaxation of ^{59}Co in a single crystal of $\text{K}_3\text{Co}(\text{CN})_6$

M. J. R. Hoch*

Department of Physics, University of the Witwatersrand, Johannesburg, South Africa

J. A. J. Lourens† and M. I. Gordon

Department of Physics, University of South Africa, Pretoria, South Africa

(Received 7 July 1975)

NMR spin-lattice relaxation-time measurements have been carried out for ^{59}Co in a single crystal of $\text{K}_3\text{Co}(\text{CN})_6$ over the temperature range from 77 to 308 K. The results suggest that an internal optical mode of the $\text{Co}(\text{CN})_6$ octahedron, with wave number 412 cm^{-1} , is primarily responsible for relaxation. A detailed quadrupolar relaxation calculation based on a point-charge model provides support for this conclusion. It is believed that this is the first situation in which such a relatively high-frequency mode has been found to be of dominant importance in nuclear relaxation.

I. INTRODUCTION

Nuclear spin-lattice relaxation via quadrupolar processes in ionic crystals containing complex anions has provided information on the lattice dynamics and structures of these substances. Recently, for example, Armstrong and Jeffrey¹ and Van Driel *et al.*² have studied K_2PtX_6 compounds and have established the importance of the rotary lattice mode, involving PtX_6 octahedra, in the relaxation of X ($X = \text{Cl}, \text{Br}$) nuclei. Van Driel *et al.*² were able to follow the softening of this mode near a phase transition in K_2PtBr_6 .

There appears to have been no previous NMR relaxation-time investigation of M nuclei in a substance of the type $R_3M(\text{YZ})_6$. In this paper relaxation measurements for ^{59}Co nuclei in a single crystal of $\text{K}_3\text{Co}(\text{CN})_6$ are reported over the temperature range 78–304 K. The initial motivation for this work came from cw studies³ of the temperature dependence of the ^{59}Co quadrupolar coupling constant, which suggested that a rotary lattice mode of wave number $\sim 25\text{ cm}^{-1}$ played a dominant role in averaging the electric field gradient at the cobalt site. This mode has not been found to be of importance for relaxation, and it appears that an internal optical mode of the $\text{Co}(\text{CN})_6$ octahedron with wave number 412 cm^{-1} is primarily responsible for relaxation between 100 and 304 K. Other internal modes with lower wave numbers $\sim 100\text{ cm}^{-1}$ apparently play a negligible role in relaxation in this temperature region. In an effort to understand this result we have carried out a detailed calculation using the general approach of Van Kranendonk.⁴ The details and conclusions are presented in Secs. III and IV.

II. MEASUREMENTS

The single-crystal sample of the diamagnetic complex $\text{K}_3\text{Co}(\text{CN})_6$ was grown from solution. Previous work⁵ has established that this type of crystal is polytypic and the sample used had an orthorhombic unit cell containing four nonequivalent Co nuclei. X-ray and cw NMR measurements^{3,6} have shown that the $\text{Co}(\text{CN})_6$ octahedron is slightly distorted (D_{3h} symmetry) giving rise to a static electric field gradient (efg) at the Co site. The present measurements, which were made at 10.5 MHz (10.4 kG) using a conventional coherent pulsed NMR spectrometer, involve only the central component of the quadrupole split spectrum. The crystal was oriented with its c -axis perpendicular to the magnetic field and was then rotated about this axis until the central components (two pairs of almost coincident lines) coincided. This was sensitively achieved by observing the beats on the free-induction decay (FID) and setting for zero beat. All measurements refer to this orientation. Temperatures could be controlled and measured to within 1 K.

Since the spacings of the energy levels are not equal it may be expected that relaxation will be nonlinear. This is further discussed in Sec. III. In the experiment the populations of $+\frac{1}{2}$ and $-\frac{1}{2}$ states were equalized (maximum FID) using an rf pulse whose length was about a quarter of the length of a 90° pulse for cobalt ions in solution. This agrees closely with the value calculated using a fictitious spin- $\frac{1}{2}$ approach.⁷ Recovery of the magnetization was studied in the usual way using a second pulse of the same length. No departure from single-relaxation time behavior could be detected for pulse spacings up to twice the

apparent relaxation time. We shall, however, refer to our measured values as the initial relaxation times. The repetition rate was kept low to allow the system to recover completely.

The signal to noise ratio was approximately unity at room temperature and therefore digital signal averaging was employed. The signals from the rf phase detector were digitized with a Biomation 610A transient recorder which was interfaced⁸ to the direct memory access channel of a Nova 1220 computer. The system is capable of digitizing signals at a sampling rate of up to 10 MHz in sweeps of 128 points and up to 3500 sweeps sec^{-1} . Accuracy of the measured T_1 values is estimated to be better than 10%.

III. RELAXATION THEORY

Since the spacings of the Co energy levels are not equal (Sec. II) it is not possible to use the Hebel-Slichter relationship,⁹ which is based on the spin-temperature concept, to obtain an expression for T_1 ($1/T_1 = W_1 + W_1' + W_1'' + 4W_2 + 4W_2' + 4W_2''$). Instead we have written down the rate equations for the populations of the various states. Fig. 1 defines the various transition probabilities and these are explicitly calculated below. Defining the population difference $N_4 = n_5 - n_4$, where n_5 and n_4 are the numbers of spins in levels $+1/2$ and $-1/2$ respectively, we obtain

$$\frac{dN_4}{dt} = -N_4(W_1 + W_2 + W_2') + N_3(W_1 - W_2) + N_2W_2' + 4N_0W_2 - 2N_0W_1 - 4N_0W_2', \quad (1)$$

where $N_0 = \frac{1}{2}(N_s \hbar \omega_0 / kT)$. N_s is the total number of spins and ω_0 is the Larmor frequency. [In obtain-

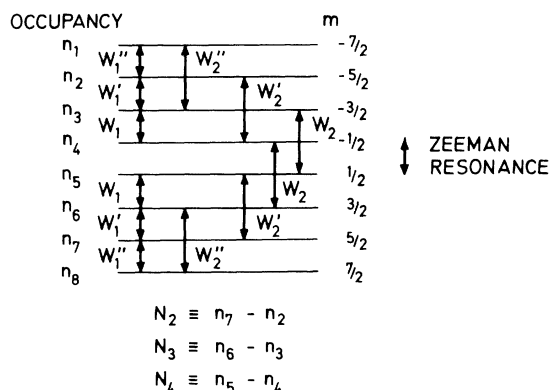


FIG. 1. Energy-level diagram for a spin- $\frac{7}{2}$ nucleus situated in a magnetic field. Quadrupolar shifts which are ignored in this scheme would give rise to unequal spacings of the levels. The transition probabilities per unit time between the various states are denoted W_1 , W_2 , etc.

ing Eq. (1) the downward transition probabilities are weighted with a Boltzmann factor and the quadrupole interaction is assumed small compared to the Zeeman interaction.] Similar expressions are obtained for the other population differences and in order to obtain an expression for N_4 it is necessary to solve four simultaneous differential equations. Since experiment shows that relaxation is approximately governed by a single exponential (Sec. II) we simply calculate the initial relaxation rate given by

$$1/T_1 \approx W_1 + W_2 + W_2'. \quad (2)$$

Andrew and Tunstall¹⁰ have given a theoretical discussion of quadrupolar relaxation for an $I = \frac{5}{2}$ system and have presented their results graphically for various W_1/W_2 ratios. The recovery behavior of the central component depends on the initial conditions and calculations were carried out for two cases. For the case of initial saturation of the central component only, recovery appears to approximately follow a single exponential. Similar behavior may be expected for an $I = \frac{7}{2}$ system. Narath¹¹ has treated the case of magnetic relaxation ($\Delta m = \pm 1$) for an $I = \frac{7}{2}$ system. Again, for the case of initial saturation of the central component, he finds that recovery is governed by a single exponential over the first decade but with an apparent relaxation time substantially shorter than $1/2W_1$. Our assumption concerning the relaxation rate is consistent with these analyses.

For this system spin-lattice relaxation via lattice vibrations may in principle involve the acoustic modes or optical modes such as the rotary-lattice mode and the internal modes of the $\text{Co}(\text{CN})_6$ octahedron. In Sec. IV it is shown that the acoustic modes make a negligible contribution and it is thus necessary to obtain an expression for T_1 involving the optical mode contributions. Our calculation is similar to that of Armstrong and Jeffrey,¹ who considered a spin- $\frac{3}{2}$ system in an NQR experiment, but our final result is somewhat different. The basic approach is due to Van Kranendonk⁴ and Kochelaev.¹²

Assuming that only Raman processes need be considered the transition rates occurring in Eq. (2) may be written

$$W_{m, m+\mu} = \frac{2\pi}{\hbar} \sum_{II'} \sum_{\vec{k}\vec{k}'} |\langle m + \mu, n_{\vec{k}'I'} + 1, n_{\vec{k}I} - 1 | \mathcal{C}_Q | m, n_{\vec{k}'I'}, n_{\vec{k}I} \rangle|^2 \times \delta(E_{m+\mu} + E_{\vec{k}'I'} - E_m - E_{\vec{k}I}), \quad (3)$$

where m denotes the initial spin state and $m + \mu$ the final spin state ($\mu = \pm 1, \pm 2$). $n_{\vec{k}I}$ denotes the

number of phonons with wave vector \vec{k} in optical branch l and $E_{\vec{k}l} = \hbar\omega_l(\vec{k})$ is the phonon energy. The summations are over all branches and wave vectors. The quadrupolar Hamiltonian \mathcal{H}_Q may be written⁷

$$\mathcal{H}_Q = \sum_{\mu=-2}^2 F^\mu Q^\mu, \quad (4)$$

where F^μ represents a lattice operator and Q^μ a spin operator. In the Van Kranendonk⁴ approach F^μ is expanded in terms of lattice displacements and only the second-order term is retained. This may be written $\sum_{i\alpha\beta} u_{i\alpha} A_{ii,\alpha\beta}^\mu u_{i\beta}$ where $u_{i\alpha}$ is the α th component of the relative displacement of two atoms i and o given by $\vec{u}_i = \vec{r}_i - \vec{r}_o$. The elements of the tensors A_{ii}^μ have been tabulated by Van Kranendonk for crystals of the NaCl type in a point charge approximation and they may be taken over directly for an octahedral structure. The $u_{i\alpha}$ may be expanded in terms of the normal modes in the harmonic approximation¹³ and one obtains

$$\begin{aligned} \sum_{i\alpha\beta} u_{i\alpha} A_{ii,\alpha\beta}^\mu u_{i\beta} \\ = \frac{\hbar}{2N} \sum_{\substack{i\vec{k} \\ i\vec{k}'}} \chi_i^\mu(\vec{k}\vec{k}', l l') \frac{[a(\vec{k}, l) + a^\dagger(-\vec{k}, l)]}{\omega_l(\vec{k})^{1/2}} \\ \times \frac{[a(\vec{k}', l') + a^\dagger(-\vec{k}', l')]}{\omega_{l'}(\vec{k}')^{1/2}}, \end{aligned} \quad (5)$$

where

$$\begin{aligned} \chi_i^\mu(\vec{k}\vec{k}', l l') = \sum_{\alpha\beta} A_{ii,\alpha\beta}^\mu \left[\frac{e_{i\alpha}(\vec{k}, l)}{m_i^{1/2}} - \frac{e_{o\alpha}(\vec{k}, l)}{m_o^{1/2}} \right] \\ \times \left[\frac{e_{i\beta}(\vec{k}', l')}{m_i^{1/2}} - \frac{e_{o\beta}(\vec{k}', l')}{m_o^{1/2}} \right]. \end{aligned} \quad (6)$$

The sum over i includes all neighbors (mass m_i) of the atom o containing the resonant nucleus which is Co in this case. For reasons discussed in Sec. IV in summing over i , we shall only consider the nearest-neighbor C atoms. The $a(\vec{k}, l)$ and $a^\dagger(-\vec{k}, l)$ are phonon annihilation and creation operators. $e_{i\alpha}(\vec{k}, l)$ is the displacement eigenvector for the i th atom along direction α during execution of the normal mode of wave vector \vec{k} , branch l . N is the number of unit cells in the crystal.

Combining Eqs. (4) and (5) with (3) gives

$$\begin{aligned} W_{m, m+\mu} = \frac{2\pi}{\hbar} |\langle m+\mu | Q^\mu | m \rangle|^2 \\ \times \sum_{\substack{i\vec{k} \\ i\vec{k}'}} \left| \sum_i \chi_i^\mu(\vec{k}\vec{k}', l l') \right|^2 (n_{\vec{k}l} + 1) n_{\vec{k}'l} \\ \times \delta(\hbar\omega_o + \hbar\omega_{\vec{k}l} - \hbar\omega_{\vec{k}'l}), \end{aligned} \quad (7)$$

where $\hbar\omega_o = E_{m+\mu} - E_m$. The spin operator matrix elements are standard.¹⁴ In order to proceed it is necessary to make certain assumptions and these are detailed below. We assume (i) that the optical branches do not overlap and each optical branch may be considered separately ($l=l'$), (ii) the eigenvectors $e_{i\alpha}(\vec{k}, l)$ may be taken to be independent of \vec{k} ,¹² and (iii) a linear dispersion relation may be used¹²

$$\omega_l(k) = \omega_{l0} - \Delta\omega_l(k/k_m), \quad (8)$$

$\Delta\omega_l$, which is the bandwidth of mode l , is assumed small, as implied by assumption (i), so that

$$\omega_l(k) \simeq \omega_l(k') \simeq \omega_{l0}.$$

Replacing the summations over $\vec{k}\vec{k}'$ by integrals and approximating the first Brillouin zone by a sphere gives

$$\begin{aligned} W_{m, m+\mu} = \frac{\pi^3}{160} |\langle m+\mu | Q^\mu | m \rangle|^2 \\ \times \sum_{l l'} \frac{|\sum_i \chi_i^\mu(l l')|^2}{\Delta\omega_l \omega_{l0}^2 \sinh^2(\beta\hbar\omega_{l0}/2)}, \end{aligned} \quad (9)$$

where

$$\begin{aligned} \chi_i^\mu(l l') = \sum_{\alpha\beta} A_{ii,\alpha\beta}^\mu \left(\frac{e_{i\alpha}(l)}{m_i^{1/2}} - \frac{e_{o\alpha}(l)}{m_o^{1/2}} \right) \\ \times \left(\frac{e_{i\beta}(l')}{m_i^{1/2}} - \frac{e_{o\beta}(l')}{m_o^{1/2}} \right). \end{aligned} \quad (10)$$

Equation (9) shows that if $\Delta\omega_l$ is small the transition rate is high. This is because of the high density of states in this case. Relaxation can, of course, only occur if $\Delta\omega_l$ is greater than the Zeeman splitting. This condition is well satisfied in NMR experiments.

Combining Eq. (9) with Eq. (2) gives

$$\frac{1}{T_1} = \frac{9}{16} \pi^3 \left(\frac{eQ}{2I(2I-1)} \right)^2 \frac{R^l}{\Delta\omega_l \omega_{l0}^2 \sinh^2(\beta\hbar\omega_{l0}/2)}, \quad (11)$$

where

$$R^l = \sum_{l l'} \left| \sum_i \chi_i^l(l l') \right|^2 + 7 \sum_{l l'} \left| \sum_i \chi_i^2(l l') \right|^2. \quad (12)$$

The summations over $l l'$ in Eq. (12) refer to degenerate branches of a mode of given frequency as implied by assumption (i) above. Calculation of the $\chi_i^l(l l')$ and $\chi_i^2(l l')$ involve the quantities

$$A_{ii}^1 = \frac{eS}{16a_o^5} \begin{pmatrix} 0 & 0 & e'_i \\ 0 & 0 & f'_i \\ e'_i & f'_i & 0 \end{pmatrix}, \quad (13a)$$

and

$$A_{it}^2 = \frac{es}{16a_{oi}^5} \begin{pmatrix} a_i & d_i & 0 \\ d_i & b_i & 0 \\ 0 & 0 & c_i \end{pmatrix}, \quad (13b)$$

where the elements are given numerically by Van Kranendonk.⁴ The quantity a_{oi} is the spacing between atoms o and i and s is a factor which takes into account shielding, overlap, etc. The effects of anharmonic Raman processes are briefly mentioned in Sec. IV.

IV. DISCUSSION

The experimental T_1 data are shown as plotted points in Fig. 2 in a log-log plot vs $T(K)$. As discussed in Secs. II and III the T_1 values represent the initial relaxation times. For a Debye model of the acoustic lattice modes Van Kranendonk⁴ has shown that

$$1/T_1 \propto T^{*2} E(T^*), \quad (14)$$

where $T^* = T/\Theta_D$, Θ_D being the Debye temperature. $E(T^*)$ is a function which increases as T^{*5} for $T < 0.02\Theta_D$ and which approaches unity for $T \sim \Theta_D$. For $K_3Co(CN)_6$, $\Theta_D \approx 290$ K,¹⁵ and the relaxation-rate contribution due to acoustic modes may be expected to follow a T^2 law for $T \geq 100$ K. This clearly does not fit the data and shows that acoustic modes are unimportant in relaxation. This is not unexpected since the efg at the Co site is primarily produced by the ligand CN groups within the $Co(CN)_6$ octahedron and their contribution is not modulated by acoustic modes.

We next briefly consider the rotary-lattice mode³ of wave number 25 cm^{-1} . Equation (11) predicts that this mode should give rise to a temperature dependence of T_1 represented by a dashed curve in Fig. 2, where again the curve is drawn to pass through points near 300 K. This does not fit the results. The contribution due to this mode is estimated theoretically later in this section.

The best fit full curve drawn through the experimental points has the form $T_1 = 0.06 \sinh^2(600/2kT)$ corresponding to a mode of wave number 412 cm^{-1} with an uncertainty of about 10%. This result implies that one or more intermediate-frequency internal optical modes of the $Co(CN)_6$ octahedron are primarily responsible for relaxation in the range $100 < T < 300$ K. We consider the contributions of these modes in detail below.

Degeneracies reduce the 33 normal modes of the octahedron to 13. (This ignores the small distortion of the octahedron from O_h symmetry mentioned in Sec. II, which will lift the degeneracy

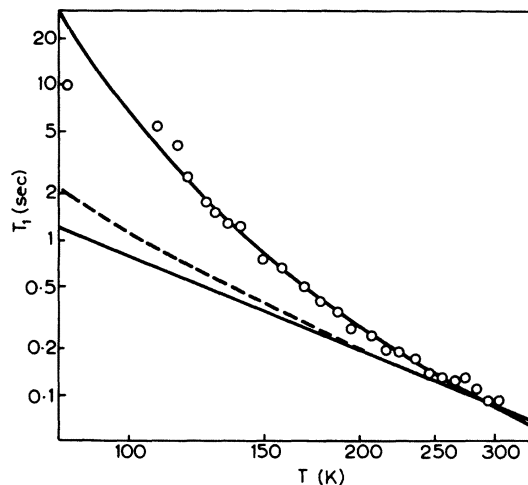


FIG. 2. $\log_{10} T_1$ vs $\log_{10} T$ for ^{59}Co in $K_3Co(CN)_6$. The circles are experimental points. The lower solid curve shows a T^2 dependence while the upper solid curve is a best fit curve corresponding to a wave number of 412 cm^{-1} . The dashed curve shows the temperature dependence to be expected if the rotary-lattice mode of wave number 25 cm^{-1} were important in relaxation.

somewhat.) In order to compare the contributions of the various modes it is necessary to determine the eigenvectors $e_{i\alpha}(l)$ involved in Eq. (11). We note that T_1 depends rather sensitively on the $e_{i\alpha}(l)$. Before doing this and obtaining numerical values for the R^l defined in Eq. (12), for each mode, some general remarks are made. A point-charge approach is adopted and we assume that the efg at the Co site arises solely from the six nearest-neighbor C atoms. This is a reasonable approximation since it has been shown¹⁶ that these atoms contribute about 90% of the static efg due to the CN ligands. (A relaxation mechanism of the type proposed by Wikner, Blumberg, and Hahn,¹⁷ which takes into account the efg fluctuations due to dipole moments induced by the optical vibrations, has not been considered because of the small C atom polarizability.)

Four modes give zero contribution. These are the two A_{1g} modes Q_1 and Q_2 and the two E_g modes Q_3 and Q_4 . The only modes which involve Co atom motions are the four F_{1u} modes Q_6 , Q_7 , Q_8 , and Q_9 . Since Q_6 is a high frequency mode (2129 cm^{-1}) it may be expected to make a negligible contribution at the temperatures of interest. There are thus only eight triply degenerate modes for which calculations must be carried out.

For the F_{1g} and F_{2g} modes Q_5 , Q_{10} , and Q_{11} the following expression is obtained for R^l

$$R^{F_{1g}} = 8856 e_C^4, \quad (14a)$$

while for the F_{2u} modes Q_{12} and Q_{13} we obtain

$$R^{F_{2u}} = 45\,144e_C^4, \quad (14b)$$

where e_C is the eigenvector for the C-atom motions. For the F_{1u} modes Q_8 and Q_9 the expression is

$$\begin{aligned} R^{F_{1u}} = & 72\,576(e'_C \pm ke_{Co})^4 + 45\,144(e_C \mp ke_{Co})^4 \\ & + 385\,344(e'_C \pm ke_{Co})^2(e_C \mp ke_{Co})^2 \\ & + 69\,120(e_C \mp ke_{Co})^3(e'_C \pm ke_{Co}), \end{aligned} \quad (14c)$$

where the upper signs apply to Q_8 and the lower signs to Q_9 . For Q_7 an almost identical expression applies except that all signs are positive apart from that in front of the final term which is negative. e'_C is the eigenvector amplitude for the C atoms which move collinearly with e_{Co} , e_C refers to the other four C atoms and $k = (m_C/m_{Co}) \approx 1/\sqrt{5}$. The eigenvectors for all atoms in an octahedron are of course normalized for each mode and this is mentioned below.

The calculation of the eigenvectors may be carried out using infrared and Raman spectroscopic results together with the standard procedures of molecular spectroscopy.¹⁸ Jones,^{19,20} and Nakagawa and Shimanouchi²¹ have given G and F matrices appropriate to this situation where G is the kinetic-energy matrix and F is the force-constant matrix in terms of symmetrized internal coordinates. The L matrix has been obtained by diagonalizing the GF matrix based on the elements of Jones²⁰ and normalizing according to the relation $LL^T = G$. The columns of the L matrix give the eigenvectors in terms of internal coordinates (bond bending and stretching) and from these the Cartesian displacement eigenvectors may be determined. The displacements are similar to those given by Jones, McDowell and Goldblatt²² for other hexacarbonyls.

Table I gives the R^I values calculated using Eqs. (14a), (14b), and (14c) for the eight modes of interest together with spectroscopically assigned wave numbers.^{20,23} For the rotary-lattice mode Q_0 of wave number $\sim 25\text{ cm}^{-1}$ we estimate that $R^{Q_0} \leq 1$ for the slightly distorted octahedron. (An

undistorted octahedron would give $R^{Q_0} = 0$.) At high temperatures ($\beta\hbar\omega_{i0} \sim 1$) we may write approximately

$$\frac{1}{T_1^I} \propto \left(\frac{R^I}{\omega_{i0}^4 \Delta\omega_I} \right) T^2. \quad (15)$$

Table I together with Eq. (15) suggests that certain F_{1u} and F_{2u} modes should play a dominant role in relaxation. Unfortunately the $\Delta\omega_I$ are not known at all reliably. However, the low-frequency ($\sim 100\text{-cm}^{-1}$) modes may be expected to be strongly coupled to the lattice modes and consequently to have larger bandwidths than intermediate-frequency ($\sim 400\text{-cm}^{-1}$) modes. Comparing the F_{1u} and F_{2u} modes we see that for Q_8 to be dominant $\Delta\omega_{Q_{13}} > 5\omega_{Q_8}$. Similarly, in comparing the F_{1u} modes Q_8 and Q_9 we find that for Q_8 to be dominant, $\Delta\omega_{Q_8} > 7\Delta\omega_{Q_9}$ if we use the frequencies assigned by Nakagawa.²³ These results are not unreasonable. While $R^{Q_7} \sim 2R^{Q_8}$ this is offset by the population factor. We conclude that the point-charge calculation offers substantial evidence that Q_8 is the mode responsible for relaxation.²⁴ The spectroscopically assigned frequency for Q_8 is in agreement with the best fit frequency of 412 cm^{-1} obtained from Fig. 2.

Finally we comment on the quantitative agreement of theoretical and experimental T_1 values. For definiteness we shall consider the contribution of Q_8 but the calculation may be readily extended to several nonoverlapping modes. Assuming a bandwidth of 5 cm^{-1} and a R^{Q_8} value of 7000 gives $T_1 \sim (4 \times 10^3)/s^2$ at 300 K. Comparison with the data of Fig. 2 gives $s \sim 200$, which is not unusual for point-charge quadrupolar relaxation calculations. Clearly, the inclusion of other modes will reduce this value somewhat. If anharmonic Raman processes are taken into account by incorporating microscopic Gruneisen parameters into Eq. (11), this may result in a further reduction in the theoretical T_1 values. The predicted temperature dependence will, however, remain unchanged.

TABLE I. Relaxation contributions due to various internal modes of the $\text{Co}(\text{CN})_6$ octahedron. R^I is defined in the text. The eigenfrequencies in parentheses are tentative assignments or calculated values given by the authors referred to.

Representation	F_{1g}	F_{1u}	F_{1u}	F_{1u}	F_{2g}	F_{2g}	F_{2u}	F_{2u}
(Mode)	Q_5	Q_7	Q_8	Q_9	Q_{10}	Q_{11}	Q_{12}	Q_{13}
Eigenfrequency	Ref. 20 [358]	564	416	[84]	[480]	98	[440]	[72]
ω_I (cm^{-1})	Ref. 23 [303]	565	414	129	[450]	129	[380]	100
R^I	170	14 300	7100	450	360	20	1700	130

V. CONCLUSION

Analysis of ^{59}Co NMR spin-lattice relaxation time measurements in $\text{K}_3\text{Co}(\text{CN})_6$ suggests that intermediate frequency ($\sim 400\text{ cm}^{-1}$) internal modes of the $\text{Co}(\text{CN})_6$ octahedron dominate in relaxation. A detailed point-charge quadrupolar relaxation calculation, which takes into account the contributions of the various internal modes, substantially supports this conclusion and shows that one of the F_{1u} modes (Q_8) is likely to be of dominant importance in relaxation. The present work has

shown that nuclear relaxation can provide information on the internal dynamics of ionic complexes if the probe nucleus occupies a central position, of high symmetry, in the complex.

ACKNOWLEDGMENTS

We should like to thank Dr. E. C. Reynhardt for providing the crystal used in the measurements, Dr. A. G. Every for useful discussions, and Professor R. L. Armstrong for helpful comments on the manuscript.

*Work supported by the Solid State Physics Research Unit of the University of the Witwatersrand and the South African Council for Scientific and Industrial Research.

†Work supported by the South African Council for Scientific and Industrial Research and the University of South Africa.

- ¹R. L. Armstrong and K. R. Jeffrey, *Can. J. Phys.* **49**, 49 (1971).
- ²H. M. Van Driel, M. Wiszniewska, B. M. Moores, and R. L. Armstrong, *Phys. Rev. B* **6**, 1596 (1972).
- ³J. A. J. Lourens and E. C. Reynhardt, *Phys. Status Solidi A* **12**, 215 (1972).
- ⁴J. Van Kranendonk, *Physica (Utr.)* **20**, 781 (1954).
- ⁵J. A. Kohn and W. D. Townes, *Acta. Crystallogr.* **14**, 617 (1961).
- ⁶E. C. Reynhardt and J. C. A. Boeyens, *Acta. Crystallogr. B* **28**, 525 (1972).
- ⁷A. Abragam, *Principles of Nuclear Magnetism* (Oxford U. P., London, 1961), Chaps. 2 and 8.
- ⁸Details of the interface circuitry are available on request from M. I. Gordon.
- ⁹C. P. Slichter, *Principles of Magnetic Resonance* (Harper and Row, New York, 1963), p. 120.
- ¹⁰E. R. Andrew and D. P. Tunstall, *Proc. Phys. Soc. Lond.* **78**, 1 (1961).
- ¹¹A. Narath, *Phys. Rev.* **162**, 320 (1967).
- ¹²B. I. Kochelaev, *Zh. Eksp. Teor. Fiz.* **37**, 242 (1959) [*Sov. Phys.-JETP* **10**, 171 (1960)].
- ¹³A. A. Maradudin, E. W. Montroll, and G. H. Weiss, *Solid State Physics Supplement 3* (Academic, New York, 1963), Chap. 1.
- ¹⁴M. H. Cohen and F. Reif, *Solid State Physics* **5**, 332 (Academic, New York, 1957).
- ¹⁵T. H. Chou, S. L. McBride, and N. Rumin, *Can. J. Phys.* **49**, 1597 (1971).
- ¹⁶J. A. J. Lourens and E. C. Reynhardt, *Advances in NQR* **1**, 315 (Heyden, London, 1974).
- ¹⁷E. G. Wikner, W. E. Blumberg, and E. L. Hahn, *Phys. Rev.* **118**, 631 (1960).
- ¹⁸E. B. Wilson, Jr., J. C. Decius, and P. C. Cross, *Molecular Vibrations* (McGraw-Hill, New York, 1955), Chap. 6.
- ¹⁹L. H. Jones, *J. Mol. Spectr.* **8**, 105 (1962).
- ²⁰L. H. Jones, *J. Chem. Phys.* **41**, 856 (1964).
- ²¹I. Nakagawa and T. Shimanouchi, *Spectrochim. Acta.* **18**, 101 (1962).
- ²²L. H. Jones, R. S. McDowell, and M. Goldblatt, *Inorg. Chem.* **8**, 2349 (1969).
- ²³I. Nakagawa, *Bull. Chem. Soc. Jpn.* **46**, 3690 (1973).
- ²⁴A preliminary account of this work has appeared elsewhere: M. I. Gordon, M. J. R. Hoch, and J. A. J. Lourens, *Proceedings of the Eighteenth Ampere Congress*, edited by P. S. Allen, E. R. Andrew, and C. A. Bates, Nottingham, 1974 (unpublished). Certain of the calculations presented there have now been shown to be incorrect.